Nonspecific protein adsorption on cationically modified Lyocell fibers monitored by zeta potential measurements

Claudia Payerl[1,2], Matej Bračič[3], Armin   Zankel[4], Wolfgang J. Fischer[2,5], Manuel Kaschowitz[1], Eleonore Fröhlich[6], Rupert Kargl[1,3], Franz Stelzer[1], Stefan Spirk[1,2,3,5]*

[1]*Institute for Chemistry and Technology of Materials, Graz University of Technology, Stremayrgasse 9, 8010 Graz, Austria.*

[2]*CD-Laboratory for Fiber Swelling and Paper Performance, Inffeldgasse 23(A), 8010 Graz, Austria*

[3]*Laboratory for Characterization and Processing of Polymers (LCPP), University of Maribor, Smetanova 17, 2000 Maribor, Slovenia.*

[4]*Graz Centre of Electron Microscopy, and Institute of Electron Microscopy, Graz University of Technology, Steyrergasse 17, 8010 Graz, Austria*

[5]*Institute for Paper, Pulp and Fiber Technology, Inffeldgasse 23, 8010 Graz, Austria*

[6]*Center for Medical Research, Medical University of Graz, Stiftingtalstraße 24, Graz, Austria*

Members of the European Polysaccharide Network of Excellence (EPNOE).

To whom correspondence should be addressed:

* E-Mail: stefan.spirk@tugraz.at, Tel.:+43 316 873 32284.

26 **Abstract**

27

28 Nonspecific protein deposition on Lyocell fibers via a cationization step was explored by

29 adsorption of two different *N,N,N*-trimethyl chitosan chlorides (TMCs). The cationization and

30 the subsequent protein deposition steps were performed and monitored *in situ* by evaluating

31 the zeta potential using the streaming potential method. Both employed TMCs (degree of

32 substitution with N^+Me_3Cl groups: 0.27 and 0.64) irreversibly adsorbed on the fibers as

33 proven by charge reversal (-12 to +7 mV for both derivatives) after the final rinsing step.

34 Onto these cationized fibers, BSA was deposited at different pH values (4, 5, and 7). Charge

35 titrations revealed that close to the isoelectric point of BSA (4.7), BSA deposition was

36 particularly favored, while at lower pH values (pH 4), hardly any adsorption took place due to

37 electrostatic repulsion of the cationic fibers and the positively charged BSA.

38

39 **Keywords:** Lyocell fibers, protein adsorption, zeta potential, tenacity, chitosan

40

41 **Highlights:**

42

43 - Interaction capacity of Lyocell fibers with N,N,N-trimethylchitosan chloride and BSA.

44 - The adsorption behavior is monitored online by zeta potential determinations.

45 - As complementary techniques, charge titrations and low-voltage SEM are used.

46 - Mechanical properties of the fibers are studied before and after adsorption.

47

48

49

50

51

1. Introduction

The immobilization of functional layers on cellulosic surfaces has seen a tremendous increase of research activities over the past two decades. One emerging area has been the equipment of cellulosic materials with biomolecules.(Hasani, Cranston, Westman, & Gray, 2008; Mohan et al., 2014; Mohan, Ristic, et al., 2013) In terms of applications, the main motivation is to generate biocompatible, potentially implantable cellulose-based biosensors.(Kargl et al., 2013; Hannes Orelma, Filpponen, Johansson, Laine, & Rojas, 2011; Hannes; Orelma, Johansson, Filpponen, Rojas, & Laine, 2012) In this context, cellulose offers an advantage such as a rather low nonspecific binding of proteins which allows for selective anchoring of bioactive molecules in a physiological environment.(Filpponen et al., 2012) Previous studies on different types of cellulosic materials revealed that bovine serum albumin (BSA), a widely used marker to assess nonspecific binding, hardly adsorbs on cellulosic materials.(Hannes Orelma et al., 2011) This behavior originates from several factors, namely the amphiphilic nature of cellulose, combined with its rather high degree of swelling, hampering nonspecific binding since both, the highly hydrated cellulosic material and the protein, need to be dehydrated upon interaction.(Norde & Lyklema, 1991) Further, BSA and other nonspecific markers mainly adsorb nonspecifically via hydrophobic interactions.(Roach, Farrar, & Perry, 2005, 2006)

For many applications, the interaction capacity of proteins must be controlled in order to achieve a controllable device. In this context, several different approaches do exist which use either chemical grafting of functional groups or simple physical adsorption of biocompatible species such as other polysaccharides for instance.(Kargl et al., 2012; Liu, Choi, Gatenholm, & Esker, 2011; Miletzky et al., 2015; Mishima, Hisamatsu, York, Teranishi, & Yamada, 1998; Mohan, Zarth, et al., 2013; Taajamaa, Rojas, Laine, Yliniemi, & Kontturi, 2013) Depending on the isoelectric point (IP) of the chosen protein and the adsorption conditions

77   (pH, temperature, ionic strength), either negatively or positively charged polysaccharides can

78   be employed to tune the amount of deposited proteins. In this context, carboxymethyl

79   celluloses, cationic celluloses and chitosans have been reported in literature, whereas in most

80   cases thin films have been studied.(Hasani et al., 2008; Hannes Orelma et al., 2011; Salas,

81   Rojas, Lucia, Hubbe, & Genzer, 2013; Strasser et al., 2016) The advantage of thin films is

82   their rather uniform appearance in terms of morphology, porosity and chemical composition.

83   Further, surface sensitive methods do exist to monitor the adsorption behavior of such

84   biomolecules in real time such as quartz crystal microbalance with dissipation (QCM-D) and

85   surface plasmon resonance (SPR). The 2D confinement of such films can give rise to basic

86   interaction capacities of cellulose with such biomolecules but the rather complex morphology

87   and porosity of real fiber samples make direct comparisons difficult or even impossible to

88   establish. On the other hand, there are only limited tools available to study the adsorption of

89   biomolecules on fibers *in situ* and most papers deal with the *ad mortem* analysis of the

90   samples after adsorption has been completed revealing the kinetics unexplored. One of the

91   few methods capable to monitor changes in real time on fibers is to follow the change in the

92   zeta potential of the fibers during the adsorption using the streaming potential

93   method.(Jacobasch, 1989) This method exploits changes in the charge of the samples upon

94   adsorption and allows for the analysis of interaction capacities and to investigate adsorption

95   processes of a wide range of materials with cellulose fibers ranging from inorganic clays to

96   synthetic polymers and biopolymers such as chitosan, carboxymethyl cellulose and proteins

97   for instance. Most biomolecules are charged and therefore such experiments can be employed

98   to gain insights into their interaction capacity with cellulosic fibers by evaluation of the

99   change in zeta potential during the adsorption.(Hubbe, Rojas, Lucia, & Jung, 2007; Ribitsch,

100   Stana-Kleinschek, Kreze, & Strnad, 2001; Ristić, Hribernik, & Fras-Zemljič, 2015; K. Stana-

101   Kleinschek & Ribitsch, 1998; L. Zemljič, Peršin, Stenius, & Kleinschek, 2008)

4

102   In this study, we aim at a detailed investigation of biomolecule adsorption on cellulosic fibers

103   by monitoring the change in zeta potential. As model system, we employ regenerated

104   cellulose staple fibers (Lyocell) which are coated with *N,N,N*-trimethyl chitosan chlorides

105   (TMC) having different degrees of substitution. Afterwards, BSA adsorption at different pH

106   values is performed. All these coating experiments are performed *in situ* using the streaming

107   potential method and characterization is further complemented by low voltage scanning

108   electron microscopy (LV-SEM) and charge titration studies after the adsorption experiments

109   have been completed. Mechanical properties were investigated in order to track changes

110   induced by the adsorbed polysaccharide and the subsequent protein layer.

111

112   **2. Materials and Methods**

113   2.1 Materials

114   *N,N,N*-trimethyl chitosan chloride (TMC, M_w: 50 – 80 kDa, medical grade) with two different

115   degrees of substitution (TMC$_L$: Degree of acetylation: 0.2, Degree of substitution (DS): with

116   NMe$_3^+$Cl$^-$: 0.27; TMC$_H$: Degree of acetylation: 0.32, Degree of substitution (DS) with

117   NMe$_3^+$Cl$^-$: 0.64) was purchased from Kitozyme S.A. (Herstal, Belgium). Aqueous TMC

118   solutions (0.1 g/mL) were prepared and the pH value was adjusted to seven using HCl and

119   NaOH (0.1 M).

120   Lyocell staple fibers (trade name TENCEL Standard) were kindly provided by Lenzing AG,

121   Austria. The titer and the length of the fibers were 1.3 dtex and 3.8 mm, respectively.

122   BSA was purchased from Sigma-Aldrich, Austria, and used as received. BSA solutions (c =

123   0.1 g/mL) at pH 4.0, 5.0 and 7.0, were prepared in 10 mM KCl aqueous solution with MilliQ

124   water (resistivity 18 MΩ cm). The pH value was adjusted by adding 0.1 M NaOH or 0.1 M

125   HCl solution.

126 2.2 Surface modification of cellulose fibers with TMC

127 In the first step, cellulose fibers were rinsed with 500 mL electrolyte solution (conductivity ~

128 16 mV) to remove fiber finishing agents. After the rinsing step, a 10 mM KCl electrolyte

129 solution was adjusted to pH 7, injected into the system and a baseline of pure cellulose was

130 recorded in the zeta potential measurements. TMC (0.1 g/ mL) was subsequently dissolved in

131 the electrolyte solution and the *in-situ* adsorption thereof was again recorded using the zeta

132 potential. All experiments have been performed in three repetitions.

133 2.3 BSA adsorption on TMC- modified cellulose fibers

134 BSA adsorption onto the modified and non-treated fibers was studied at pH values of 4, 5 and

135 7 in 10 mM KCl electrolyte solution (c_{BSA} = 0.1 mg/mL). The adsorption process was

136 monitored until an adsorption plateau was observed and then the system was rinsed with the

137 respective electrolyte solution to remove loosely bound BSA molecules. All experiments have

138 been performed in three repetitions.

139 2.4 Zeta potential measurements/ electrokinetic measurements

140 The Streaming Potential was recorded using the SurPASS, an Electro kinetic Analyzer

141 (Anton Paar GmbH, Graz, Austria,) and the resulting zeta potential was calculated according

142 to the Smoluchowski, equation 1. The SurPASS is equipped with Ag/AgCl- electrodes which

143 are continuously determining the streaming potential. The sample was applied as a fiber plug

144 between two perforated electrodes using the equipped cylindrical cell of the instrument which

145 allows for measuring fluid streaming through the fiber plug and the detection of the potential.

146

147 The zeta potential ζ was calculated according to Smoluchowski (1)

148 $$\zeta = \frac{dU}{dp} \times \frac{\eta}{\varepsilon_r \times \varepsilon_o} \times \kappa \quad (1)$$

149

150   where U is the streaming potential, p is the pressure, ε_r is the relative permittivity of the fluid

151   and ε_0 the dielectric constant and the vacuum permittivity, η is the viscosity and κ the

152   conductivity of the fluid.(Delgado et al., 2005) The pH-dependence of zeta potential was

153   determined in the presence of 10 mM KCl solution. If the properties of the liquid phase

154   remain constant, the electrokinetic potential of fibers is influenced by several parameters:

155   chemical constitution, polarity of the surface region, microstructure of the fiber, such as

156   porosity and crystallinity, and swelling properties in water.

157   2.5 Tensile testing

158   The tenacity (cN/dtex) and elongation at break (%) of single Lyocell fibers including blank

159   samples were determined according to ISO 5079 using a Vibroskop 400 (Lenzing Technik

160   Instruments) under defined conditions (50% humidity, 25°C). Gauge length, pre-loading and

161   cross-head speed were 20 mm, 70 mg, 20 mm/min, respectively. 20 fibers for each sample

162   were tested.

163

164   2.6 Low voltage scanning electron microscopy (LVSEM)

165   While conventional scanning electron microscopy (CSEM) uses an electron beam with a

166   landing energy of the electrons between 5 and 30 keV for imaging, the so-called low voltage

167   scanning electron microscopy (LVSEM) is performed at energy values between 0.5 and 5

168   keV.(Reimer, 1993) Since the penetration depth of the electrons into the specimen is smaller

169   at lower energies the resolution of surface details is enhanced.(Joy & Joy, 1996) Additionally,

170   this mode enables imaging of the neat surface of an electrically non-conducting specimen

171   without any additional layer produced by e.g. carbon or gold coating, which is prerequisite at

172   CSEM. Imaging of non-conductive specimens without charging can only be realized at

173 special energy values which are material specific and can be found in literature.(Goldstein et

174 al., 2003; Joy & Joy, 1996; Reimer, 1993) Furthermore potential beam damage caused by the

175 electron beam may be lowered and artefacts produced during preparation are avoided.

176 In this investigation, a beam energy of 0.65 keV was applied for imaging, a value which

177 performed well for cellulose fibers.(Fischer et al., 2014) The Everhart-Thornley detector of

178 the scanning electron microscope Zeiss ULTRA 55 (Carl Zeiss Micro Imaging GmbH,

179 Germany) delivered images with topographic contrast using secondary electrons

180 (SE).(Goldstein et al., 2003)

181 2.7 Charge titrations

182 The pH-dependent potentiometric titrations were performed on TMC coated fibers by

183 dissolving a 180 mg sample in 30 ml of Milli-Q water having very low carbonate ion content.

184 Boiling of water and subsequent cooling under nitrogen gas is the preferable method to

185 achieve a carbonate ion content of less than 10^{-6} mol/ L. The solution was titrated in a forward

186 (from acidic to alkaline) and backward (alkaline to acidic) manner from pH = 3 to pH = 11

187 using 0.1 M hydrochloric acid and 0.1 M potassium hydroxide. The KCl concentration of the

188 solution was 10 mM. The titrants were added to the system in a dynamic mode using a double

189 burette Mettler Toledo T70 automatic titration unit. The pH value was measured with a

190 Mettler Toledo InLab Routine L combined glass electrode. Charges were calculated as

191 published elsewhere.(L. F. Zemljič, Čakara, Michaelis, Heinze, & Stana Kleinschek, 2011)

192

193 2.8 Cytoxicity testing and screening of eluates/extracts

194 The extraction was carried out in compliance with ISO10993-5 and ISO 10993-12

195 regulations.(ISO, 2007, 2009) Eluates were prepared by incubation of 0.2 g fibres per ml cell

196 culture medium (Minimum Essential Medium (MEM) + 10% fetal bovine serum (FBS),

8

197 PAA) for 72±1h at 37±1°C. Eluates were centrifuged at 10.000 rpm for 10 min to remove

198 fibres and the supernatants used for the testing.

199 MRC-5 cells (American Type Culture Collection, CCL-171™) were cultured in MEM + 10%

200 FBS and subcultured in regular intervals. For the testing, 80.000 cells were seeded per well to

201 obtain the required cell density (subconfluent condition) and treated the following day with

202 pure eluates and dilutions of the eluates of 1:2, 1:5, 1:10 and 1:20 for 24 h. Treatment with

203 50% ethanol/50% Triton X100 served as positive (toxic) control and the extraction medium

204 was the negative control. The detection with the CellTiter 96® Aqueous Non-Radioactive

205 Cell Proliferation Assay (Promega) uses a novel tetrazolium compound (3-(4,5-

206 dimethylthiazol-2-yl)-5-(3-carboxymethoxyphenyl)-2-(4-sulfophenyl)-2H-tetrazolium, inner

207 salt; MTS) and an electron coupling reagent (phenazine methosulfate; PMS). The MTS

208 solution and the PMS solution were thawed, 100 µl of the PMS solution was mixed with 2 ml

209 of MTS solution and 20 µl of the combined MTS/PMS solution was added to 100 µl of each

210 well. Plates were incubated for 2 h at 37±1°C and 5% CO_2 in a cell incubator. Absorbance

211 was read at 490 nm on a plate reader (SPECTRA MAX plus 384, Molecular Devices). In

212 parallel, cells were viewed by bright-field microscopy to confirm the MTS data.

213 Dehydrogenase activity (DHA) as indication for cell viability was calculated according to the

214 Eq. 1:

215

216 $DHA(\%) = 100 \times (A_{490nm}sample - A_{490nm}blank) / (A_{490nm}control - A_{490nm}blank)$ (Eq. 1)

217

218 Indication for cytotoxic effect according to European and American guidelines for biological

219 evaluation of medical devices is a dehydrogenase activity of less than 70% compared to

220 untreated controls (solvent controls).(ISO, 2009)

221

222 The ISO 10993-5 guideline for cytotoxicity advocates the use of a standard, fully

223 characterized, cell line for cytotoxicity testing. L929 cells were one of the first cells

224 established in 1940 and are still the most commonly used cells for cytotoxicity testing

225 according to ISO 10993 guidelines.(Earle et al., 1943) MRC-5 cells are of human origin and

226 were established around 30 years later.(Jacobs, Jones, & Baille, 1970) Several publications

227 suggest that human and rodent primary cells and cell lines derived from both species are

228 equally suitable for the prediction of lethality.(Halle & Spielmann, 1992; NIEHS, 2001)

229 Cytotoxicity testing according to ISO10993 did not reveal decrease in viability upon

230 incubation of cells with eluates of Tencel + TMC for 24h, while viability of cells incubated

231 with the positive control was $6 \pm 0\%$. This finding was confirmed by the similar cell densities

232 seen in negative control and wells exposed to the eluates and cell loss in the positive control.

233

234 **3. Results and Discussion**

235 In the first step, exhaustively rinsed cellulose fibers were subjected to a flow of TMC

236 solutions having two different DS_{NMe3Cl} (0.64 and 0.27, respectively, denoted as TMC_H and

237 TMC_L in the following) at pH 7 in 10 mM KCl. The adsorption experiments are designed as

238 follows: under a constant flow the adsorbate is pumped through the fibers under constant

239 pressure ($p=$ 200 mbar) and after the adsorption step, the fibers are rinsed with the electrolyte

240 solution in order to remove loosely bound material. As expected, both TMC derivatives

241 render the negatively charged cellulose fiber (ca. -15 mV) cationic, whereas a plateau is

242 reached after about 300 seconds (Figure 1).

243
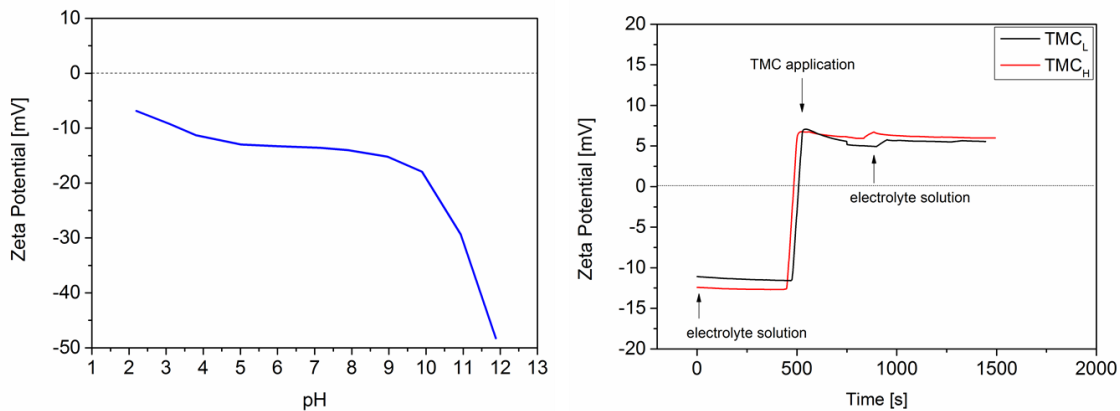
Figure 1. Comparison of the pH dependent zeta potential (via the streaming oscillation method) of Lyocell fibers (left) and zeta potential of fibers coated with TMC_L and TMC_H as a function of time (right, pH 7, c= 0.1 g/L, 10 mM KCl). All experiments have been performed in three repetitions.

Remarkably, both zeta potential curves have an identical shape indicating spontaneous adsorption. The rinsing step does not induce a significant negative change in zeta potential, which demonstrates the irreversibility of the TMC adsorption. However, swelling also impacts the absolute values of the zeta potential and therefore the amount of adsorbed charged species may vary although their zeta potential is essentially identical. Interestingly, there is not any major difference in the absolute zeta potential between highly and lowly substituted derivatives, after adsorption onto the fibers (+7 mV, Figure 1). On first glance, this points at a significantly higher amount of TMC with the lower DS on the fibers which is required to compensate for the charges of the negatively charged cellulose fibers. Though, the contribution of the free primary amine groups to the observed zeta potential is negligible since at pH 7 these groups are hardly protonated.(Ristić et al., 2014)

The charge titration results yield a more differentiated picture. For the TMC_L coated fibers, a lower amount of charges (54 mmol/kg) has been identified whereas for the fibers treated with TMC_H, 78 mmol/kg fibers were determined. However, a limitation of these titrations is their sensitivity to dissociable/protonable groups, such as primary amines and carboxylic acids. When comparing the amount of free amine groups in both derivatives (0.5 vs 0.04 for TMC_L

11

265 and TMC$_H$, respectively) it becomes evident that a larger amount of TMC$_H$ must be located

266 onto the fibers. These results are further supported by LV-SEM. The presence of both TMC

267 derivatives on the fibers was not only revealed by charge titration and zeta potential

268 determinations but also verified by LV-SEM images (Figure 2). The topographic contrast of

269 the SEM shows comparatively large aggregates of a coating on the TMC$_H$ samples.
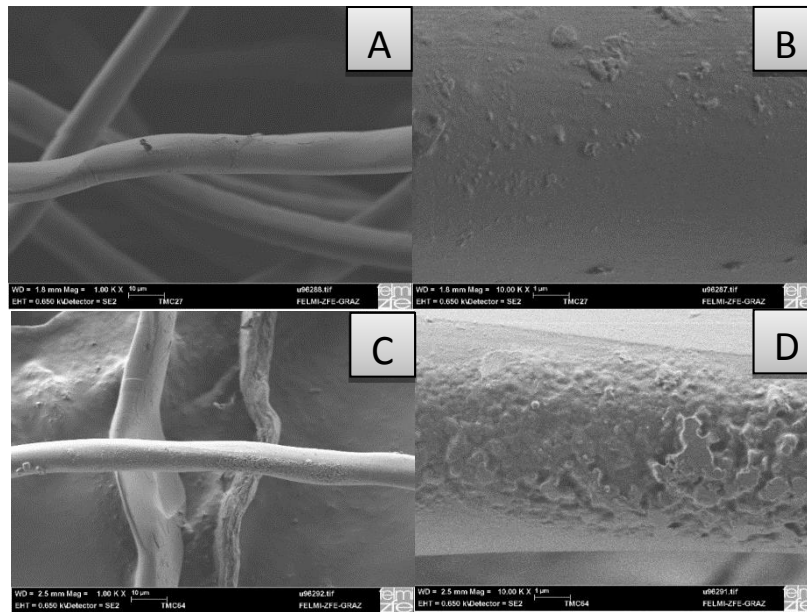
270

271 Figure 2. Comparison of the LV-SEM images at different magnifications of the
272 different TMC coated fibers. TMC$_L$: A: 1000x, B: 10000x, TMC$_H$ C: 1000x; D:
273 10000x
274

275 These results showcase a specifity of zeta potential measurements in particular and

276 electrokinetic phenomena in general since the obtained potentials cannot be directly correlated

277 to the amount of material on a given substrate. Factors like accessibility (void volume) and

278 swelling lead to shifts in the shear plane, consequently impacting zeta potentials. (Karin

279 Stana-Kleinschek, Kreze, Ribitsch, & Strnad, 2001) In this context, it seems plausible that the

280 TMC$_H$ layer causes more swelling, resulting in a lower effective zeta potential than the TMC$_L$

281 modified fibers.

282

283 3.1 Adsorption of BSA

284 Like already reported several times, BSA does not significantly adsorb on neat cellulose

285 materials.(Lavenson, Tozzi, McCarthy, Powell, & Jeoh, 2011) Figure 3 shows that neither at

286 pH 5 nor 7 any significant amounts of BSA remained on the cellulose surface after the rinsing

287 step.
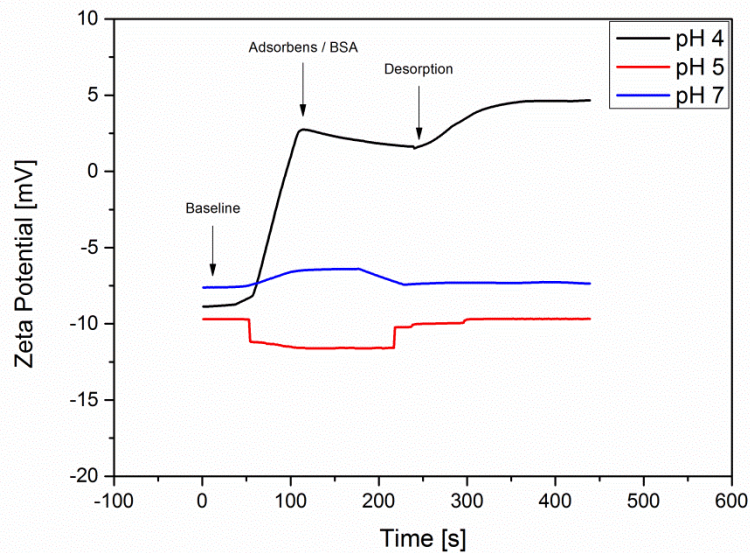
288

289 Figure 3. BSA Adsorption on unmodified Lyocell fibers at different pH values monitored by
290 zeta potential measurements. All experiments have been performed in three repetitions.
291

292 At pH 4, BSA adsorption takes place due to electrostatic forces between the positively

293 charged BSA and the negatively charged cellulose fiber surface. In contrast, after successful

294 coating with TMC and subsequent cationization of the fibers, the adsorption of BSA on the

295 fibers is substantially increased, whereas the extent of adsorption relates to the pH value

296 where the adsorption had been performed.

297 We have to distinguish different cases and their effects on the zeta potential since BSA is

298 negatively charged above its isoelectric point (4.7) at a pH value of 5, and positively charged

299 below its IP.(Norde & Lyklema, 1991) The easiest case is adsorption at a pH value of 7 since

300 any type of BSA adsorption would be indicated by a decrease of the zeta potential, and, if the

301 charge of the TMC was compensated, a negative zeta potential would be observed, which is

302 indeed observed (Figure 4).

13
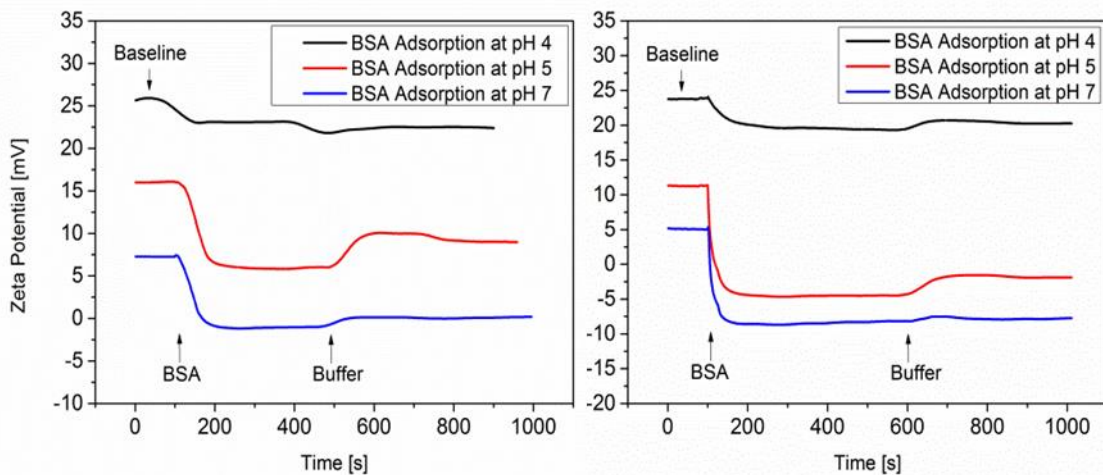
Figure 4. Zeta potential as a function of time during the adsorption of BSA on TMC_L (left) and TMC_H, (right). All experiments have been performed in three repetitions.

The zeta potential changes from +6 mV for the TMC_H coated fiber at pH 7 to ca -8 mV, which approximately corresponds to the zeta potential of BSA at pH 7 in a 10 mM KCl solution which is an indication for a complete coverage of the surface with BSA (Salgin, Salgin, & Bahadi, 2012). On the other hand, it can be clearly seen that less BSA adsorbs onto the TMC_L coated samples at pH 7 since the offered charge by the TMC_L is just sufficient to achieve charge complexation and a zeta potential of close to 0 mV results.

For the other pH values, the situation is much more complex since the resulting zeta potential is influenced by two factors, namely the contribution of the primary amine groups, which are protonated at pH 4 and 5 respectively, as well as the change in the net charge of the BSA which causes as zeta potential of zero at pH 5 and +5 mV at pH 4.(Salgin et al., 2012) Therefore, even before adsorption of BSA at pH 4 and 5, the zeta potentials of the TMC coated fibers are higher than at pH 7 due to the contribution of the protonated primary amine groups. However, although the zeta potential is similar for both TMC derivatives at pH 4 (+26 vs +24 mV) and 5 (12 vs 16 mV), respectively, there are distinct differences during and after BSA adsorption. First, the TMC_H derivative promotes to a much larger extent the BSA

14

322   deposition compared to the TMC_L. At pH 5 for instance, the zeta potential is close to zero

323   after BSA adsorption for the TMC_H coated cellulose sample. This means that the charge of

324   the TMC_H has been completely neutralized whereas on TMC_L BSA adsorbs to a much lesser

325   extent, indicated by a still positive zeta potential of + 7 mV.

326   In contrast, at a pH value of 4, where BSA is positively charged (in 10 mM KCl solution,

327   BSA features a zeta potential of ca +7 mV), differences between the two TMC samples are

328   less pronounced. Since the zeta potential is lower for BSA than for the TMC coated surfaces,

329   a deposition of the BSA would result in a reduction of the potential if it was mainly

330   influenced by the outer BSA layer. Such a decrease is actually observed for both TMC coated

331   samples albeit the decrease is rather small (from +24 to +22 mV) pointing at a rather low

332   adsorption of the positively charged BSA onto the positively charged fibers. Interestingly, the

333   kinetics of the BSA adsorption is differing significantly for the two TMC derivatives. It can

334   be clearly seen in Figure 4 that the deposition of BSA on the TMC_L coated fibers proceeds

335   much slower than on the TMC_H coated samples. A closer look on the zeta potential

336   experiments at pH 5 reveals that the zeta potential is zero at that pH value for TMC_H while for

337   TMC_L it is still positive. This means that in the case of TMC_H, BSA covers the surface and

338   the zeta potential is dominated by the net charge of the outermost layer consisting of BSA

339   molecules having zero net charge. On the contrary, for TMC_L, a (sub)monolayer like

340   arrangement cab be assumed at pH 5, since the surface still exhibits a positive zeta potential

341   after the exposure to BSA. Similar differences are even more pronounced at pH 7. While for

342   the adsorption of BSA on thin films decorated with TMC there has not been a significant

343   difference between the differently charged TMC derivatives in terms of affinity towards BSA,

344   the fibrous materials show some trend. The TMC_H coated fibers are clearly more prone to

345   BSA adsorption than the TMC_L coated ones. The negative zeta potential is an indication that

346   BSA is present in excess on TMC_H coated fibers whereas the rather neutral zeta potential for

347   TMC_L coated materials may be caused by charge neutralization with BSA.

The interaction mechanism of BSA on TMC coated viscose fibers depends on the charge density of the substrate, as well as on the charge of the protein under investigation, here BSA, and its solubility. The solubility is a key driver in the deposition of any type of substance since the solubility in close spatial proximity to the interface is further reduced compared to freely rotating molecules, which are not translationally constrained by an interface. At pH 5, where BSA has its solubility minimum, the highest impact of the coating on the promotion of BSA deposition was observed by zeta potential monitoring. However, it turned out that the charge density of the surfaces is a crucial parameter too. We already demonstrated at the example of thin mostly amorphous cellulose films using QCM-D and SPR measurements that the adsorption of BSA is more pronounced on those substrates which have been rendered with TMC and cationic cellulose derivatives having a higher DS than on those with a lower DS.(Mohan, Ristic, et al., 2013) In these papers, the highest deposition was observed at pH 5 for both samples, whereas we speculated that the driving force was of electrostatic nature. This observation is on first glance contradictory since the net charge of BSA at pH 5 is close to zero but this just means that there is an equal amount of positively and negatively charged groups available. However, the negatively charged domains are capable to interact with the positively charged support and this effect is stronger the higher the charge density of the substrate is. As we showed here by charge titrations, the charge density is much higher on TMC_H coated fibers than those on TMC_L, which translates to a higher amount of deposited polymer. Consequently, a stronger impact on the zeta potential for the TMC_H coated samples is observed. Charge titration studies confirm the larger amount of BSA on the TMC_H treated surfaces since the charge density is nearly twice as high as for the TMC_L coated cellulose fibers (268 mmol/kg vs. 122 mmol/kg). Since the charges on the TMC_H should not significantly change upon adsorption of BSA, its increase must be related to the amount of deposited BSA on the TMC coated fibers, (Table 1).

Table 1. Charges and zeta potential difference Δζ of BSA coated fibers, obtained by charge titration and streaming potential. The Δζ is the potential jump from the start-potential of the adsorption to the end-potential after rinsing and desorption. Please note that in the charge titrations only dissociable groups contribute (e.g. NH_2 and COOH).

|	Charge [mmol/kg] TMC$_L$	Charge [mmol /kg] TMC$_H$	Δζ [mV] TMC$_L$	Δζ [mV] TMC$_H$
Coated fibers	54	78	7	7
BSA/ pH 4	50	40	3	4
BSA/ pH 5	122	268	7	13
BSA/ pH 7	80	100	7	13

It should be noted at this point that even the final fibrous products (BSA on TMC coated Lyocell fibers) are non-cytotoxic. This was validated using MRC-5 human cells which revealed that after exposing the cells to the material there was not any reduction in viability of the cells compared to the control. Detailed results on cell viability are given in the Supplementary Material (Figure S1).

3.2 Mechanical properties

For many applications, the influence of coatings on the mechanical performance of fibers is a crucial issue since they impact the final material's performance. In this context, all the samples have been subjected to testing concerning tenacity and elongation at break. Figure 5 shows the tenacity of the TMC coated fibers, which is higher than those of the non-treated fibers and which increase with increasing charge density of the TMC. This is in line with other reports, where an increase in charge density was associated in higher strength of

390   cellulosic materials. This has been often interpreted as if charge density and presumably

391   cross-linking by ionic bonds or by other forces is a decisive factor for increasing the

392   resistance against elastic deformation.(Aarne, Vesterinen, Kontturi, Seppälä, & Laine, 2013)

393   In the case of TMC, the significance of these differences in tenacity was evaluated by a t-Test

394   using an α-value of 95% for the statistical calculations. The p-values were calculated and

395   significant differences were observed between the washed Lyocell fibers, depicted as

396   reference, and the TMC_H coated fibers. Referring as to the TMC_L coated fibers any significant

397   differences ($p > 0.05$) were not observed. A reinforcing effect of TMC coating would be

398   beneficial in many applications such as in membrane technology, textiles and composites.

399   However, the amount of deposited TMC_L is obviously too low to have a strong impact on the

400   mechanical properties. Nevertheless, it can be expected that if TMC_H reveals a reinforcing

401   effect, also TMC_L does when deposited at higher amounts.
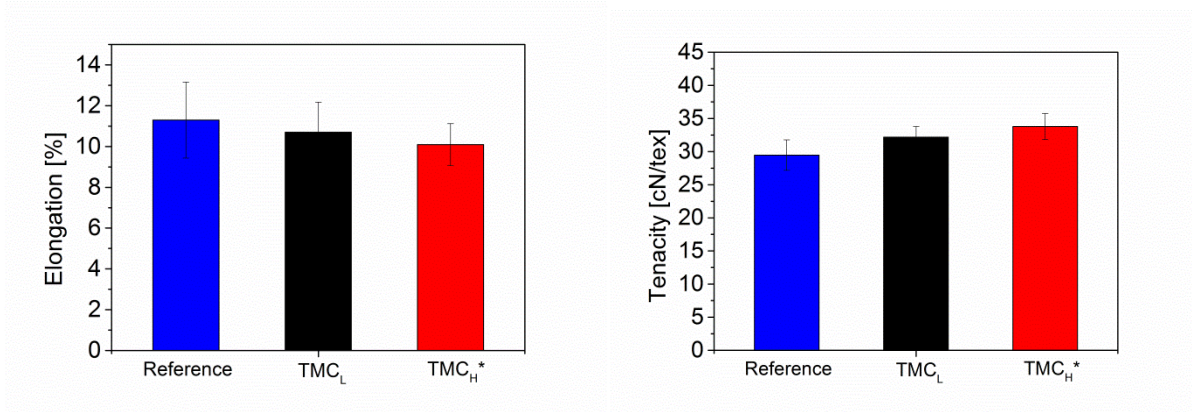

402

403 Figure 5. Comparison of tensile properties of TMC coated fibers to neat cellulose fibers
404 (denoted as reference). For each mechanical test, at least 20 fibers have been used. The
405 asterisk denotes to a statistically significant difference in respect to the reference fiber
406 samples.

407

408   Upon adsorption of BSA at different pH values, different trends are observed, and weak

409   correlation between BSA deposition and the mechanical properties could be established for

410   TMC_H coated fibers. On those fibers where a large amount of BSA is deposited (e.g. pH 5)

411   according to zeta potential and charge titration studies, the mechanical properties are similar

18

412 to untreated Lyocell fibers. In contrast, in the case hardly any protein has been adsorbed (e.g.

413 pH 4, Figure 6), TMC can execute its full potential on the reinforcing effect. Details on the

414 statistical analysis of the data can be found in the Supplementary Material (Table S1).
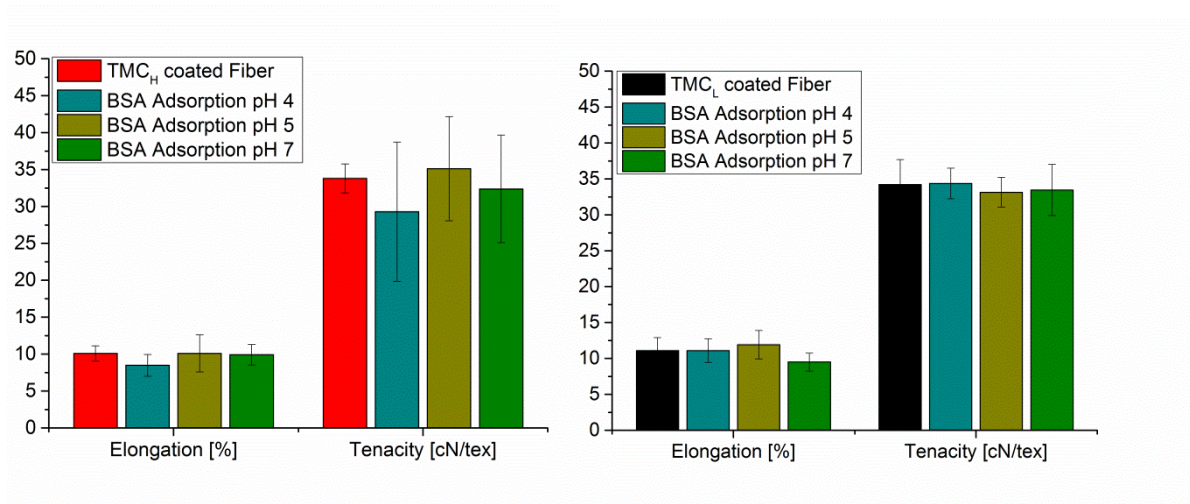
415

416 Figure 6. Comparison of tensile properties of TMC_H and TMC_L treated cellulose fibers after
417 adsorption of BSA. For each test 20 fibers have been used.
418

419

4. Summary and conclusion

421 In this paper, we demonstrated that zeta potential determinations using the streaming potential

422 method can be used to monitor protein and polymer adsorption on fibrous materials in real

423 time. It was shown that the incorporation of cationic polymers, namely *N,N,N*-trimethyl

424 chitosan chlorides, onto the fibers leads to a significant increase in the amount of deposited

425 proteins. The extent to which the proteins adsorb depends on the charge density of the

426 cationic polymer and the pH value used for the deposition. In fact, the combination of these

427 parameters allows for a tuning of the protein deposition on one hand, while the charge of the

428 resulting surface can be additionally controlled. By choosing a pH value of 5 in combination

429 with high charge density or pH 7 with low charge density, a net zero charged surface can be

430 obtained. Negatively charged surfaces are realized at pH 7 with a high amount of charges

431 whereas positively charged surfaces are obtained when a pH of 4 is used (either high or low

432 charge of TMC). It turned out that the type of TMC and subsequently low amounts of BSA

433 increase the resistance against elastic deformation of the resulting fibrous materials. However,

434 these effects are (over)compensated by the adsorption of excess BSA and highly protein

435 coated fibers show similar mechanical properties as the non-treated Lyocell fibers.

436 Still, although the zeta potential method is a potentially powerful tool to monitor adsorption

437 on surfaces, the use of additional methods is required to quantify the amount of deposited

438 polymers. If such information is available, then also the contribution of swelling and its

439 influence on the zeta potential can be determined. Subsequently, qualitative assessments on

440 the extent of swelling after the coating could be established, which are valuable parameters in

441 a variety of fiber modification processes.

442

446

447 **References**

448

449 Aarne, N., Vesterinen, A.-H., Kontturi, E., Seppälä, J., & Laine, J. (2013). A Systematic
450   Study of Noncross-linking Wet Strength Agents. *Industrial & Engineering Chemistry*
451   *Research, 52*(34), 12010-12017.
452 Delgado, A. V., Gonzalez-Caballero, F., Hunter, R. J., Koopal, L. K., Lyklema, J., Alkafeef,
453   S., Chibowski, E., Grosse, C., Dukhin, A. S., Dukhin, S. S., Furusawa, K., Jack, R.,
454   Kallay, N., Kaszuba, M., Kosmulski, M., Noremberg, R., O'Brien, R. W., Ribitsch, V.,
455   Shilov, V. N., Simon, F., Werner, C., Zhukov, A., & Zimmermann, R. (2005).
456   Measurement and interpretation of electrokinetic phenomena: (IUPAC technical
457   report). *Pure and Applied Chemistry, 77*(10), 1753-1805.
458 Earle, W., Schilling, E., Stark, T., Straus, N., Brown, M., & Shelton, E. (1943). Production of
459   Malignancy in Vitro. IV. The Mouse Fibroblast Cultures and Changes Seen in the
460   Living Cells. *Journal of the National Cancer Institute, 51*, 165-212.
461 Filpponen, I., Kontturi, E., Nummelin, S., Rosilo, H., Kolehmainen, E., Ikkala, O., & Laine, J.
462   (2012). Generic Method for Modular Surface Modification of Cellulosic Materials in
463   Aqueous Medium by Sequential "Click" Reaction and Adsorption.
464   *Biomacromolecules, 13*, 736−742.

20

Fischer, W. J., Zankel, A., Ganser, C., Schmied, F. J., Schroettner, H., Hirn, U., Teichert, C., Bauer, W., & Schennach, R. (2014). Imaging of the formerly bonded area of individual fibre to fibre joints with SEM and AFM. *Cellulose,* 21(1), 251-260.

Goldstein, J. I., Newbury, D. E., Echlin, P., Joy, D. C., Lyman, C. E., Lifshin, E., Sawyer, L., & Michael, J. R. (2003). *Scanning Electron Microscopy and X-ray Microanalysis.* (3rd ed.). New York: Kluwer Academic/Plenum Publishers.

Halle, W., & Spielmann, H. (1992). Two procedures for the prediction of acute toxicity (LD50) from cytotoxicity data. *Alternative Lab Animals,* 20, 40-49.

Hasani, M., Cranston, E. D., Westman, G., & Gray, D. G. (2008). Cationic Surface Functionalization of Cellulose Nanocrystals. *Soft Matter,* 4, 2238-2244.

Hubbe, M. A., Rojas, O. J., Lucia, L. A., & Jung, T. M. (2007). Consequences of the nanoporosity of cellulosic fibers on their streaming potential and their interactions with cationic polyelectrolytes. *Cellulose,* 14(6), 655-671.

ISO standard 10993-12 I. (2007). Biological evaluation of medical devices – Part 12: Sample preparation and reference materials. .

ISO standard 10993-5. (2009). Biological evaluation of medical devices - Part 5: Tests for in vitro cytotoxicity.

Jacobasch, H.-J. (1989). Characterization of solid surfaces by electrokinetic measurements. *Progress in Organic Coatings,* 17(2), 115-133.

Jacobs, J. P., Jones, C. M., & Baille, J. P. (1970). Characteristics of a human diploid cell designated MRC-5. *Nature,* 227, 168-170.

Joy, D. C., & Joy, C. S. (1996). Low voltage scanning electron microscopy. *Micron,* 27, 247-263.

Kargl, R., Mohan, T., Bracic, M., Kulterer, M., Doliska, A., Stana-Kleinschek, K., & Ribitsch, V. (2012). Adsorption of Carboxymethyl Cellulose on Polymer Surfaces: Evidence of a Specific Interaction with Cellulose. *Langmuir,* 28, 11440-11447.

Kargl, R., Mohan, T., Köstler, S., Spirk, S., Doliska, A., Stana-Kleinschek, K., & Ribitsch, V. (2013). Functional patterning of biopolymer thin films using enzymes and lithographic methods. *Adv. Funct. Mat.,* 23, 308-315.

Lavenson, D. M., Tozzi, E. J., McCarthy, M. J., Powell, R. L., & Jeoh, T. (2011). Investigating adsorption of bovine serum albumin on cellulosic substrates using magnetic resonance imaging. *Cellulose,* 18(6), 1543-1554.

Liu, Z., Choi, H., Gatenholm, P., & Esker, A. R. (2011). Quartz Crystal Microbalance with Dissipation Monitoring and Surface Plasmon Resonance Studies of Carboxymethyl Cellulose Adsorption onto Regenerated Cellulose Surfaces. *Langmuir,* 27(14), 8718-8728.

Miletzky, A., Punz, M., Zankel, A., Schlader, S., Czibula, C., Ganser, C., Teichert, C., Spirk, S., Zöhrer, S., Bauer, W., & Schennach, R. (2015). Modifying cellulose fibers by adsorption/precipitation of xylan. *Cellulose,* 22(1), 189-201.

Mishima, T., Hisamatsu, M., York, W. S., Teranishi, K., & Yamada, T. (1998). Adhesion of β-D-glucans to cellulose. *Carbohydr. Res.,* 308, 389-395.

Mohan, T., Niegelhell, K., Zarth, C., Kargl, R., Köstler, S., Ribitsch, V., Heinze, T., Spirk, S., & Stana-Kleinschek, K. (2014). Triggering Protein Adsorption on cationically rendered cellulose surfaces. *Biomacromolecules,* 15, 3931-3941.

Mohan, T., Ristic, T., Kargl, R., Doliska, A., Köstler, S., Ribitsch, V., Marn, J., Spirk, S., & Stana-Kleinschek, K. (2013). Cationically rendered biopolymer surfaces for high protein affinity support matrices. *Chem. Comm.,* 49, 11530-11532.

Mohan, T., Zarth, C., Doliska, A., Kargl, R., Grießer, T., Spirk, S., Heinze, T., & Stana-Kleinschek, K. (2013). Interactions of a cationic cellulose derivative with an ultrathin cellulose support. *Carbohydr. Polym.,* 92, 1046-1053.

NIEHS. (2001). Report of the international workshop on in vitro methods for assessing acute systemic toxicity. Research Triangle Park, North Carolina: NIEHS.

Norde, W., & Lyklema, J. (1991). Why proteins prefer interfaces. *J. Biomater. Sci. Polymer Edn., 2,* 183-202.

Orelma, H., Filpponen, I., Johansson, L.-S., Laine, J., & Rojas, O. J. (2011). Modification of Cellulose Films by Adsorption of CMC and Chitosan for Controlled Attachment of Biomolecules. *Biomacromolecules, 12*(12), 4311-4318.

Orelma, H., Johansson, L.-S., Filpponen, I., Rojas, O. J., & Laine, J. (2012). Generic Method for Attaching Biomolecules via Avidin-Biotin Complexes Immobilized on Films of Regenerated and Nanofibrillar Cellulose. *Biomacromolecules, 13,* 2802-2810.

Reimer, L. (1993). *Image formation in low-voltage scanning electron microscopy. .* Bellingham, Washington: SPIE-Press.

Ribitsch, V., Stana-Kleinschek, K., Kreze, T., & Strnad, S. (2001). The Significance of Surface Charge and Structure on the Accessibility of Cellulose Fibres. *Macromolecular Materials and Engineering, 286*(10), 648-654.

Ristić, T., Hribernik, S., & Fras-Zemljič, L. (2015). Electrokinetic properties of fibres functionalised by chitosan and chitosan nanoparticles. *Cellulose, 22*(6), 3811-3823.

Ristić, T., Mohan, T., Kargl, R., Hribernik, S., Doliška, A., Stana-Kleinschek, K., & Fras, L. (2014). A study on the interaction of cationized chitosan with cellulose surfaces. *Cellulose, 21,* 2315-2325.

Roach, P., Farrar, D., & Perry, C. C. (2005). Interpretation of Protein Adsorption: Surface-Induced Conformational Changes. *Journal of the American Chemical Society, 127*(22), 8168-8173.

Roach, P., Farrar, D., & Perry, C. C. (2006). Surface Tailoring for Controlled Protein Adsorption: Effect of Topography at the Nanometer Scale and Chemistry. *Journal of the American Chemical Society, 128*(12), 3939-3945.

Salas, C., Rojas, O. J., Lucia, L. A., Hubbe, M. A., & Genzer, J. (2013). On the Surface Interactions of Proteins with Lignin. *ACS Applied Materials & Interfaces, 5*(1), 199-206.

Salgin, S., Salgin, U., & Bahadi, S. (2012). Zeta Potentials and Isoelectric Points of Biomolecules: The Effects of Ion Types and Ionic Strengths. *Int. J. Electrochem. Sci., 7,* 12404-12414.

Stana-Kleinschek, K., Kreze, T., Ribitsch, V., & Strnad, S. (2001). Reactivity and electrokinetical properties of different types of regenerated cellulose fibres. *Colloids and Surfaces A: Physicochemical and Engineering Aspects, 195*(1–3), 275-284.

Stana-Kleinschek, K., & Ribitsch, V. (1998). Electrokinetic properties of processed cellulose fibers. *Colloids and Surfaces A: Physicochemical and Engineering Aspects, 140*(1–3), 127-138.

Strasser, S., Niegelhell, K., Kaschowitz, M., Markus, S., Kargl, R., Stana-Kleinschek, K., Slugovc, C., Mohan, T., & Spirk, S. (2016). Exploring Nonspecific Protein Adsorption on Lignocellulosic Amphiphilic Bicomponent Films. *Biomacromolecules, 17*(3), 1083-1092.

Taajamaa, L., Rojas, O. J., Laine, J., Yliniemi, K., & Kontturi, E. (2013). Protein-assisted 2D assembly of gold nanoparticles on a polysaccharide surface. *Chemical Communications, 49*(13), 1318-1320.

Zemljič, L., Peršin, Z., Stenius, P., & Kleinschek, K. (2008). Carboxyl groups in pre-treated regenerated cellulose fibres. *Cellulose, 15*(5), 681-690.

Zemljič, L. F., Čakara, D., Michaelis, N., Heinze, T., & Stana Kleinschek, K. (2011). Protonation behavior of 6-deoxy-6-(2-aminoethyl)amino cellulose: a potentiometric titration study. *Cellulose, 18*(1), 33-43.